CDF Note 8137

Study of Charged Particle Species Produced in Association with $\overline{B}^0$, B^-, and $\overline{B}_s^0$ Mesons in $p\bar{p}$ Collisions at $\sqrt{s} = 1.96$ TeV.

The CDF Collaboration
URL http://www-cdf.fnal.gov

(Dated: October 13, 2005)

The yields of charged kaons, pions and protons produced in association with B mesons in $p\overline{p}$ collisions at $\sqrt{s} = 1.96$ TeV are studied using 355 pb^{-1} of data collected with the CDF detector at the Fermilab Tevatron. This is the first reported measurement of these yields at a hadron collider. The B mesons are reconstructed using their semileptonic decays

$$\begin{aligned}
B^- &\rightarrow \ell^- D^0 X, D^0 \rightarrow K^-\pi^+ \\
\overline{B}^0 &\rightarrow \ell^- D^+ X, D^+ \rightarrow K^-\pi^+\pi^+ \\
\overline{B}^0 &\rightarrow \ell^- D^{*+} X, D^{*+} \rightarrow D^0\pi^+, D^0 \rightarrow K^-\pi^+ \\
\overline{B}_s^0 &\rightarrow \ell^- D_s^+ X, D_s^+ \rightarrow \phi\pi^+, \phi \rightarrow K^+K^-.
\end{aligned}$$

The $K^\pm$, $\pi^\pm$ and $p/\overline{p}$ are identified using the time of flight detector, the CDF spectrometer, and their specific ionization (dE/dx) measured in the central drift chamber. The fraction of charged kaons produced in association with B_s^0 mesons is found to be larger than the fraction produced in associaton the B^0 and B^- mesons, as expected from naive models of heavy quark hadronization. The yields of the different particle types are found to be in qualitative agreement with the simulation of B meson production in hadron collisions from the `PYTHIA` Monte Carlo, although the yields of kaons around B_s^0 mesons is found to be larger in the simulation when compared to the data. These studies are important for understanding methods of identifying the production flavor of B_s^0 mesons in analyses of flavor oscillations and CP violation in B_s^0 meson decays.

I. INTRODUCTION

Local quark flavor conservation in QCD requires that the hadronization of a bottom quark into a bound state $b\overline{q}$ meson leaves behind another light quark, q, which will usually become a valence quark in a light meson. It is this naive picture of quark fragmentation, illustrated in Figure 1, that suggests that the correlation between the charge of the light meson and the b-quark provides a way to determine the initial flavor state of the B-meson. This technique has been used successfully in the study B^0_d oscillations and CP-violation at CDF[1, 2].

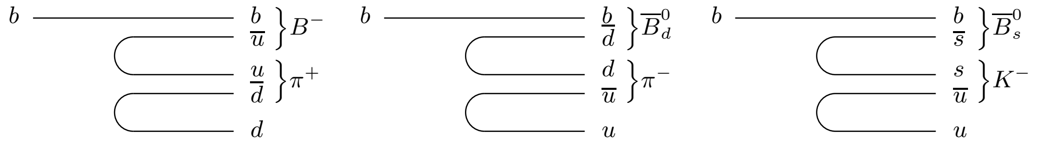

FIG. 1: Possible quark current flow diagrams illustrating the production of $\pi^{\pm}$ and K^- in association with B^-, $\overline{B}^0_d$ and $\overline{B}^0_s$ mesons.

In the case of B^- and $\overline{B}^0_d$ production, the associated light quark frequently forms a pion, but this correlation is enhanced by the presence of P-wave B-mesons that decay to $B\pi$ final states. In contrast, when a $\overline{B}^0_s$ meson is formed, the associated kaon can only be produced through the quark fragmentation process, which is currently described only by phenomenological models. The analysis described here provides the first direct observation of enhanced kaon production in association with B^0_s mesons when compared with kaon yields around B^+ and B^0_d mesons, and provides evidence to support the use of a same-side kaon tag (SSKT) in the analysis of B^0_s oscillations.

This analysis describes measurements of charged particle yields in a cone around B mesons in which time-of-flight (TOF) and ionization energy loss (dE/dx) information are used to distinguish between kaons, pions, protons and electrons. The B meson sample is obtained from the partially reconstructed semi-leptonic decays to of B-mesons to $\ell^- D^0$, $\ell^- D^+$, $\ell^- D^{*+}$ and $\ell^- D^+_s$ final states in events triggered by the presence of an electron or muon in coincidence with a track from a displaced secondary vertex. Although these final states are dominated by the decays of individual B-mesons, it is possible for B^+, B^0_d and B^0_s decays to contribute to each of the reconstructed final states. The yields of charged particles produced in association with specific B-mesons is obtained by unfolding the raw yields measured in association with ℓD final states, taking into account the relative branching ratios and reconstruction efficiencies of the individual B-decay channels.

The yields are corrected for detector acceptance, inefficiencies and decays in flight, such that the reported yields can be compared directly with predictions from Monte Carlo generators. A comparison of these yields with with those obtained using the `PYTHIA` event generator[4] is presented.

II. DATA SAMPLE AND EVENT SELECTION

This analysis was carried out using a data sample obtained from 355 pb^{-1} of $p\overline{p}$ collisions at $\sqrt{s} = 1.96$ TeV recorded with the CDF II detector[3] between April 2001 and August 2004. The data were collected using a trigger that required the presence of an electron or muon with transverse momentum (p_T) exceeding 4 GeV/c and second track with $p_T > 2$ GeV/c that was identified as being displaced with respect to the primary vertex based on the pattern of associated hits in the silicon detector.

The four semi-leptonic final final states used in this analysis were reconstructed using the decay modes

$$\begin{array}{lll} B^- & \rightarrow & \ell^- D^0 X, \quad D^0 \rightarrow K^-\pi^+ \\ \overline{B}^0 & \rightarrow & \ell^- D^+ X, \quad D^+ \rightarrow K^-\pi^+\pi^+ \\ \overline{B}^0 & \rightarrow & \ell^- D^{*+} X, \quad D^{*+} \rightarrow D^0\pi^+, \qquad D^0 \rightarrow K^-\pi^+ \\ \overline{B}^0_s & \rightarrow & \ell^- D^+_s X, \quad D^+_s \rightarrow \phi\pi^+, \qquad \phi \rightarrow K^+K^- \end{array}$$

in which the B decay that dominates each channel is indicated. Here, and throughout this note, the analysis of the these and the charge conjugate modes is implied.

Muons were identified as tracks with $p_T > 4$ GeV that extrapolated to hits in the muon chambers, while electrons were required to extrapolate to clusters of energy reconstructed in the electromagnetic calorimeter. The criteria used to reconstruct the $B \rightarrow \ell D$ decay topologies are listed in Table I. Kinematic requirements were imposed on the tracks used to reconstruct the $B \rightarrow \ell D$ decay and further requirements were imposed on the quality of a fit to this decay vertex topology. All particles used to reconstruct D-mesons were required to have transverse momenta exceeding 400 MeV/c, but more stringent requirements were imposed on the kaons used to reconstruct the D^+ and D^+_s decays. Combinations of particles that were inconsistent with the assumed decay topology were rejected based on the vertex fit χ^2. Further requirements were imposed on D-decay length measured with respect to the primary vertex in the plane transverse to the beam axis, L_{xy}, and on its significance, $L_{xy}/\sigma_{L_{xy}}$. The resolution with which the proper time of the B-decay was measured, σ_{ct}, and the proper lifetime of the D-decay, $ct(D)$, were also used to reduce backgrounds and reject poorly reconstructed B-decay candidates. The number of $B^0 \rightarrow \ell^- D^{*+} X$ decays that were mis-classified as $\ell^- D^0$ candidates was reduced by removing candidates from the $\ell^- D^0$ sample if they were also compatible with a $\ell^- D^{*+}$ final state. Finally, requirements were made on the mass of the ℓD system, the masses of intermediate states and on the helicity angle of the $\phi \rightarrow K^+K^-$ decay when reconstructing the D^+_s.

Requirement	$\ell^- D^0$	$\ell^- D^+$	$\ell^- D^{*+}$	$\ell^- D^+_s$
B vertex prob. $>$	10^{-6}	10^{-5}	10^{-6}	10^{-7}
$\chi^2_{xy}(D) <$	10	10	10	10
$L_{xy}/\sigma_{L_{xy}}(D \rightarrow PV) >$	6	11	6	5
$L_{xy}(D \rightarrow PV)$(cm) $>$	0.02	0.04	0.02	0.02
$p_T(K) >$(GeV/c)	0.4	0.7	0.4	0.6
$\sigma_{ct}(B)$(cm) $<$	0.04	0.04	0.04	0.04
$m(lD)$(GeV/c^2) $>$ to $<$	2.3 to 5.0	2.3 to 5.0	2.3 to 5.0	2.3 to 5.0
$ct(D)$(cm) $>$ to $<$	-0.015 to 0.1	-0.015 to 0.2	-0.015 to 0.1	-0.015 to 0.1
$p_T(\pi_*)$(GeV/c) $>$	-	-	0.2	-
$(m(D^*) - m(D))$(GeV/c^2) $>$ to $<$	-	-	0.1435 to 0.1475	-
$\lvert m(KK) - m(\phi_{PDG})\rvert$(GeV/$c^2$) $<$	-	-	-	0.0075
$\lvert cos(\psi)\rvert >$	-	-	-	0.2
$\chi^2_{xy}(\phi) <$	-	-	-	30

TABLE I: Selection criteria imposed on the ℓD candidates.

The yields of partially reconstructed B-decays in each channel were determined by fitting the invariant mass distribution of the D-meson candidates. The invariant mass distributions of the D-meson candidates reconstructed in both the electron and muon trigger samples is shown in Figure 2. The numbers of signal events and the signal to background ratios for the four channels reconstructed using both electrons and muons, are shown in Table II.

The different selection criteria for the individual final states produces a slightly different p_T distribution for each type of reconstructed B-decay. Since the yields of fragmentation particles produced in association with a B-meson could vary as a function of $p_T(B)$, all B-decays were re-weighted to the common p_T spectrum shown in Figure 3. This spectrum must be used when other calculations or measurements of the yields of fragmentation particles produced in association with B^0, B^+ and B^0_s mesons are compared with the results presented here.

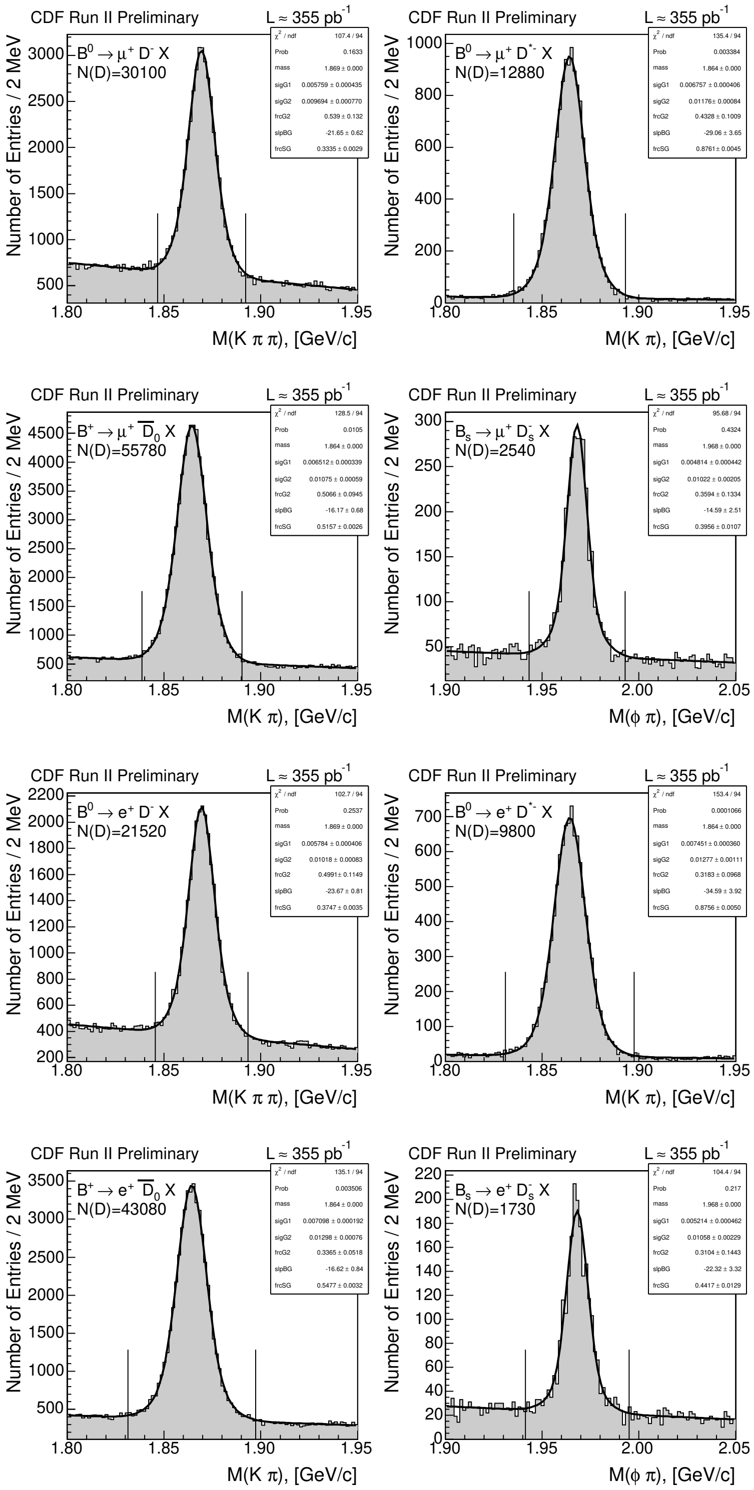

FIG. 2: Invariant mass distributions for the non-excited D states in the partially reconstructed semi-leptonic signals from electron and muon trigger samples. Vertical lines indicate the region of invariant mass used to calculate the yields and the signal-to-background ratios.

	μ+SVT		e+SVT	
	yield	S/B	yield	S/B
$\ell^- D^+$	30100 ± 293	1.6	21520 ± 257	1.8
$\ell^- D^{*+}$	12880 ± 127	18.1	9800 ± 113	16.4
$\ell^- D^0$	55780 ± 374	3.0	43080 ± 356	2.9
$\ell^- D_s^+$	2540 ± 72	2.1	1730 ± 57	2.4

TABLE II: Number of signal events and S/B for the selected ℓ+D samples.

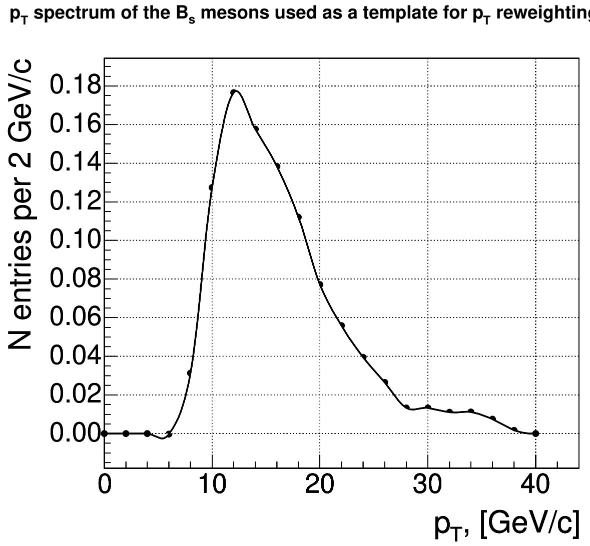

FIG. 3: Spectrum of the B meson transverse momentum to which all the reconstructed decays were re-weighted using average K-factors.

Particles produced in association with a B-decay candidate were selected if they were found within in a cone around the momentum vector of the reconstructed ℓD system based on pseudo-rapidity, η, and azimuthal angle, ϕ. Tracks with $p_T > 400$ MeV/c that were not part of the ℓD system were selected if they were within $\Delta R = \sqrt{(\Delta\eta)^2 + (\Delta\phi)^2} < 0.7$ of the ℓD momentum vector and were required to satisfy further quality criteria to allow a more direct comparison with Monte Carlo models. Specifically, the fragmentation track candidates were required to have been produced near the same primary vertex from which the B-decay candidate originated, to have been detected in at least three layers of the silicon micro-vertex detector, and to have measured impact parameters in the transverse plane consistent with being produced at the primary vertex, $|d_0|/\sigma_{d_0} < 4$. Finally, all of the selected particles were required to have associated with them both energy loss measurements and information from the TOF detector.

III. PARTICLE IDENTIFICATION

Time-of-flight (TOF) and energy loss (dE/dx) measurements were used to measure the $K^\pm$, $\pi^\pm$, $p/\overline{p}$ and $e^\pm$ fractions in the particles within the cone around B-meson candidates. An unbinned maximum likelihood fit was used to determine these fractions for five separate ranges of their transverse momentum. The D-candidate mass was used to distinguish between the ℓD signal and background with individual yields in these two classes of events determined simultaneously. The probability density for the signal, $p_S(M)$, was parameterized by two Gaussian distributions, while a linear distribution,

$p_B(M)$, in the D-candidate mass was used to describe the background. The probability density for observing a fragmentation particle candidate in one of the given p_T ranges with TOF and energy loss measurements t and dE/dx, in an event with D-candidate mass, M, is

$$P(M,t,dE/dx) = \sum_{c=S,B} P_c(M) \cdot \left(\sum_{i=\pi,K,p,e} f_c^i \cdot R_{TOF}(t - t^i_{\mathrm{exp}}) \cdot R^i_{dE/dx}(dE/dx) \right) \tag{1}$$

in which $P_c(M) = p_c(M)/(p_S(M)+p_B(M))$ are the probabilities that a D-candidate was due to signal or background and $R^i_{TOF}(t - t^i_{\mathrm{exp}})$ and $R^i_{dE/dx}(dE/dx)$ are the probability densities for a particle of type i to have a measured time-of-flight t and energy loss measurement dE/dx.

The function $R_{TOF}(t - t^i_{\mathrm{exp}})$ describes the probability of measuring a time t for a particle of type i, when the expected time is t^i_{exp}. This was parameterized by two Gaussian distributions to describe the core of the distribution, with separate exponential functions to describe positive and negative tails which contain less than 1% and 5% of the total population, respectively. The parameters in this model were determined using the known particle types in the $D^{*+} \to D^0\pi^+, D^0 \to K^-\pi^+$ decays analyzed in the $\ell^- D^{*+}$ sample. Similarly, the function $R^i_{dE/dx}(dE/dx)$ describes the probability density for a particle of type i to produce an energy loss measurement, dE/dx. The parameters used to describe these functions were determined from the analysis of dE/dx in high statistics samples of D^{*+}, $K^0_S \to \pi^+\pi^-$, $\Lambda \to p\pi^-$ decays.

The probability density in Equation 1 was used to construct an extended log-likelihood function

$$\log(L) = N\log(n) - n + \sum \log P(M,t,dE/dx) \tag{2}$$

where

$$n = \sum_{c=S,B} \sum_{i=\pi,K,p,e} n^i_c \tag{3}$$

denotes the sum of the fitted particle yields and N is the total number particles selected in the cone around the B-decay candidate. The sum extends over all selected particles in events with D-candidate mass M and with TOF and energy loss measurements t and dE/dx. From the parameters n^i_c, which maximized $\sum log(L)$, when summed over all events analysed, the fractions of each particle type in the signal and background categories were then calculated using

$$f^i_c = \frac{n^i_c}{\sum_{i=\pi,K,p,e} n^i_c}. \tag{4}$$

IV. SAMPLE COMPOSITION

The measurements of interest are the yields of kaons, pions and protons produced in association with B-mesons. However, no attempt has been made in this analysis to fully reconstruct the B decays, and each of the four ℓD final states can be produced by decays of B^+, B^0 or B^0_s. For example, Figure 4 shows the ways in which decays of B^0 and B^+ can populate $\ell^+\overline{D}^0$ and ℓ^+D^- samples via intermediate vector or P-wave D-meson states where additional particles emitted in the decay chain are not reconstructed. Given the branching ratios of all possible decay paths and with the efficiencies for each partially reconstructed final state to satisfy the selection criteria described above, it is possible to determine the multiplicities of particles produced in association with B-mesons from the measurements of the raw yields in the vicinity of the four classes of ℓD candidates using a procedure similar to ones used in previous analyses[1]. This determination also takes into account the possibility that a B-meson will decay hadronically with a lepton produced in the semi-leptonic decay of a secondary D-meson, as in $B^0 \to D^+D^-_s, D^-_s \to \ell^-\nu_\ell X$, or when a hadronic decay product of the B-meson is mis-identified as a lepton in both the trigger and offline selection.

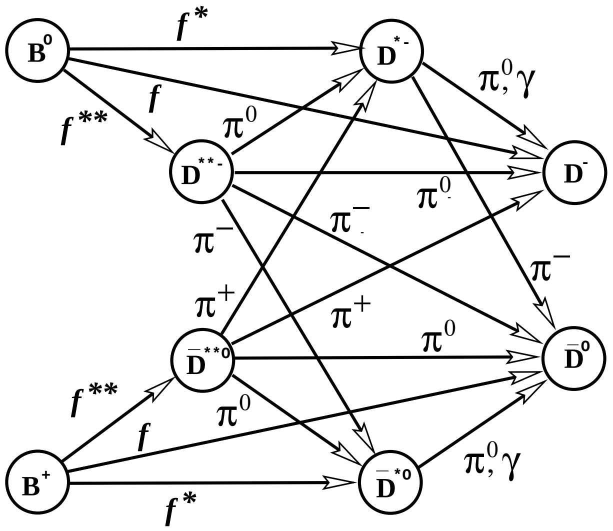

FIG. 4: The diagram illustrating the possible decay paths of B^0, B^+ mesons leading to $\ell^+\overline{D}^0$ and ℓ^+D^- final states. The lepton and neutrino are not shown.

parameter	value
f^{**}	0.31 ± 0.05
R_f	2.14 ± 0.14
P_V	0.63 ± 0.13
s	0.063 ± 0.025

TABLE III: Values of parameters used in the analysis of the B-decay sample composition.

Measurements exist[5] for the individual branching fractions for semi-leptonic B^- decays to exclusive final states containing D^0, D^{*0}, $D_1(2420)^0$, $D_2^*(2460)^0$ mesons and for semi-leptonic B^0 decays to exclusive final states containing D^+ and D^{*+} mesons. The branching fractions that have not been measured are constrained using these measured branching fractions and by isospin symmetry in terms of the probabilities f, f^* and f^{**}, that a decay proceeds directly to a ground state D-meson, or via a vector or P-wave D-meson, respectively. Rather than use these parameters, this analysis uses as inputs the quantities f^{**}, $R_f \equiv f^*/f$ and $P_V \equiv \mathrm{Br}(D^{**} \to D^*X)/\mathrm{Br}(D^{**} \to DX)$, which are more directly related to experimental measurements. Furthermore, the parameter s is used to represent the probability that a B^- or B^0 meson produces a $\ell^- D_s^+$ final state via the hadronic decay channels described above. The values of these parameters are listed in Table III.

In this way, given known multiplicities, M_i, of particles produced in association with B^-, B^0 and B_s^0 mesons, the multiplicities, m_j, found in association with each ℓD final states are given by

$$\begin{pmatrix} m_d \\ m_d^* \\ m_u \\ m_s \end{pmatrix} = \begin{pmatrix} 0.854 & 0.139 & 0.007 \\ 0.899 & 0.098 & 0.003 \\ 0.261 & 0.716 & 0.023 \\ 0.063 & 0.063 & 0.874 \end{pmatrix} \times \begin{pmatrix} M_d \\ M_u \\ M_s \end{pmatrix}. \tag{5}$$

where elements of the matrix were calculated in terms of the central values of the parameters f^{**}, R_f, P_V, s, and efficiencies determined from Monte Carlo simulations of the detector response to the individual decay modes. Since it is the multiplicities, m_j, that are measured, the multiplicities, M_i, are determined so as to minimize the quantity

$$\chi^2(\mathbf{M}) = (\mathbf{m} - \hat{\mathbf{m}}(\mathbf{M}))^T \mathbf{W}^{-1} (\mathbf{m} - \hat{\mathbf{m}}(\mathbf{M})),$$

where the expected vector of multiplicities $\hat{\mathbf{m}}(\mathbf{M})$ is calculated from $\mathbf{M}$ using Equation 5. $\mathbf{W}$ is the covariance matrix of the measured multiplicities, $\mathbf{m}$, and includes contributions from both their statistical uncertainty as well as the uncertainties on the parameters f^{**}, R_f, P_V, s. As a final step the measured yields were corrected for the possibility that unreconstructed particles produced in the B-decay chain were selected as fragmentation particle candidates. This correction reduced the total yield of pions measured in the B^0 and B^+ decays by approximately 6%.

V. RECONSTRUCTION EFFICIENCIES

The efficiency with which particles are detected by the tracking chamber in the cone around ℓD candidates was determined using a Monte Carlo simulation that modeled the semi-leptonic B-decays and detector response and emulated the behavior of the trigger. The efficiency for particles identified in this way to satisfy the remaining criteria described in Section II was determined from analysis of tracks reconstructed in the data.

Although the geometric acceptance of the tracking chambers determined in this way applies to all types of particles, a loss of efficiency unique to kaons results from decays in flight. This introduces a significant correction to observed yields of kaons which depends on their momentum and on the position in the detector at which a decay in flight occurred. Because kaons can decay at any point as they travel through the tracking chambers, they are not always lost, nor are they necessarily mis-identified as pions. These effects were studied using the detector simulation which indicated that the kaon inefficiency ranged from $21 \pm 1.5\%$ in the lowest p_T range, to $3.0 \pm 1.5\%$ in the highest. The fraction of kaons mis-classified as pions was found to be approximately 4% in all p_T ranges. Corrections for these inefficiencies and the migration of kaons into the pion classification were applied to the measured particle yields around B-mesons.

VI. SYSTEMATIC UNCERTAINTIES

The statistical uncertainties associated with the measurements of particle yields around B-mesons are due to the limited size of the ℓD samples obtained in the 355 pb^{-1} of integrated luminosity used in this analysis, and from the limited size of Monte Carlo samples used to determine the detector acceptance.

Two source of systematic uncertainty in the extracted particle yields are the imprecise determination of the parameters that describe the probability density functions for the TOF and dE/dx response and the corrections that are applied to account for decays in flight. These are referred to as correlated systematic uncertainties since they are common to yields of each type of particle produced around all B-mesons. For this reason they are quoted separately in the following sections to facilitate the comparison of kaon yields around B_s^0 and B^+/B^0 mesons.

The remaining systematic uncertainty is dominated by the imprecise measurements of branching ratios and the parameters described in Section IV that are used to characterize the sample composition. The last contribution accounts for possible deficiencies in the detector simulation used to model the performance of the tracking chamber.

VII. RESULTS

The multiplicities of $K^{\pm}$, $\pi^{\pm}$, $p/\overline{p}$ and $e^{\pm}$, and the total multiplicity of charged particles, determined from the raw yields measured around the ℓD candidates and corrected for the sample composition, detector inefficiencies and the decays of kaons, are shown in Figures 5 through 9. Figures 10,11 and 12 show the fractions of particles that are $K^{\pm}$, $\pi^{\pm}$ and $p/\overline{p}$ in the cone around B-mesons as a function of p_T. These measurements are compared with a prediction made using the `PYTHIA` Monte Carlo event generator[4] with parameters tuned so as to reproduce several characteristics of CDF data.

The relative yields of the particle species integrated over the entire p_T range from 400 MeV/c to 5 GeV/c are presented in Table IV. The errors shown are the statistical error, the correlated systematic

Relative particle yields around B candidates, data Value $\pm$ (stat.) $\pm$(common syst.) $\pm$ (syst.)			
	π,%	K,%	p,%
B^0	$81.4 \pm 0.10 \pm 1.6 \pm 0.33$	$11.6 \pm 0.25 \pm 0.34 \pm 0.085$	$5.05 \pm 0.15 \pm 0.12 \pm 0.072$
B^+	$78.9 \pm 0.12 \pm 3.1 \pm 0.35$	$12.1 \pm 0.28 \pm 0.57 \pm 0.093$	$6.70 \pm 0.17 \pm 0.22 \pm 0.077$
B_s	$71.0 \pm 0.73 \pm 1.3 \pm 1.8$	$20.2 \pm 1.2 \pm 0.59 \pm 0.29$	$6.62 \pm 0.74 \pm 0.17 \pm 0.055$
Relative particle yields around B candidates, Monte Carlo			
	π,%	K,%	p,%
B^0	84.357 ± 0.074	10.3 ± 0.15	5.05 ± 0.11
B^+	82.039 ± 0.077	11.2 ± 0.14	6.40 ± 0.11
B_s	70.24 ± 0.54	25.0 ± 0.82	4.40 ± 0.44

TABLE IV: Relative yields of charged particles in a cone around partially reconstructed B candidates.

uncertainty that is common to all B-decay modes and the weakly correlated systematic uncertainty due to the imprecisely known sample composition. Yields classified as pions also include a possible contribution from muons, which are indistinguishable from pions based on only TOF and energy loss measurements. The production of $e^{\pm}$ is dominated by Dalitz decays and secondary particles from photon conversions that satisfy the criteria intended to select only prompt tracks.

A significant enhancement in the yield of kaons produced in association with B_s^0 mesons is observed when compared with kaon yields around B^+ or B^0 mesons, as one would expect from naive models of hadronization. This trend is reproduced by the `PYTHIA` event generator, although it predicts the kaon multiplicity is to be slightly greater than what is observed in the data.

VIII. SUMMARY

The yields of charged kaons, pions, protons and electrons produced in association with B^-, B^0 and B_s^0 mesons were measured using partially reconstructed B-decays to ℓD final states. A larger yield of kaons produced in association with B_s^0 mesons is observed when compared with the yield of kaons produced in association with B^0 or B^- mesons. This trend is reproduced by the `PYTHIA` event generator, providing evidence to suggest that the charges of the excess kaons are correlated to the B_s^0 production flavor, although the level of correlation may be slightly overestimated by `PYTHIA` when run with the current set of input parameters.

Acknowledgments

We thank the Fermilab staff and the technical staffs of the participating institutions for their vital contributions. This work was supported by the U.S. Department of Energy and National Science Foundation; the Italian Istituto Nazionale di Fisica Nucleare; the Ministry of Education, Culture, Sports, Science and Technology of Japan; the Natural Sciences and Engineering Research Council of Canada; the National Science Council of the Republic of China; the Swiss National Science Foundation; the A.P. Sloan Foundation; the Bundesministerium fuer Bildung und Forschung, Germany; the Korean Science and Engineering Foundation and the Korean Research Foundation; the Particle Physics and Astronomy Research Council and the Royal Society, UK; the Russian Foundation for Basic Research; the Comisión Interministerial de Ciencia y Tecnología, Spain; and in part by the European Community's Human Potential Programme under contract HPRN-CT-20002, Probe for New Physics.

[1] CDF Collab., F. Abe, *et al.*, Phys. Rev. Lett. 80, 2057 (1998), Phys. Rev. D59, 032001 (1999).
[2] CDF Collab., T. Affolder, *et al.*, Phys. Rev. D61, 072005 (2000).
[3] F. Abe, et al., Nucl. Instrum. Methods Phys. Res. A **271**, 387 (1988); D. Amidei, et al., Nucl. Instum. Methods Phys. Res. A **350**, 73 (1994); F. Abe, et al., Phys. Rev. D **52**, 4784 (1995); P. Azzi, et al., Nucl. Instrum. Methods Phys. Res. A **360**, 137 (1995); The CDFII Detector Technical Design Report, Fermilab-Pub-96/390-E.
[4] T. Sjöstrand, *et al.*, Comp. Phys. Commun. **135**, 238 (2001); PYTHIA version 6.216 is used.
[5] K. Hagiwara *et al.*, Physical Review **D66**, 010001 (2002).

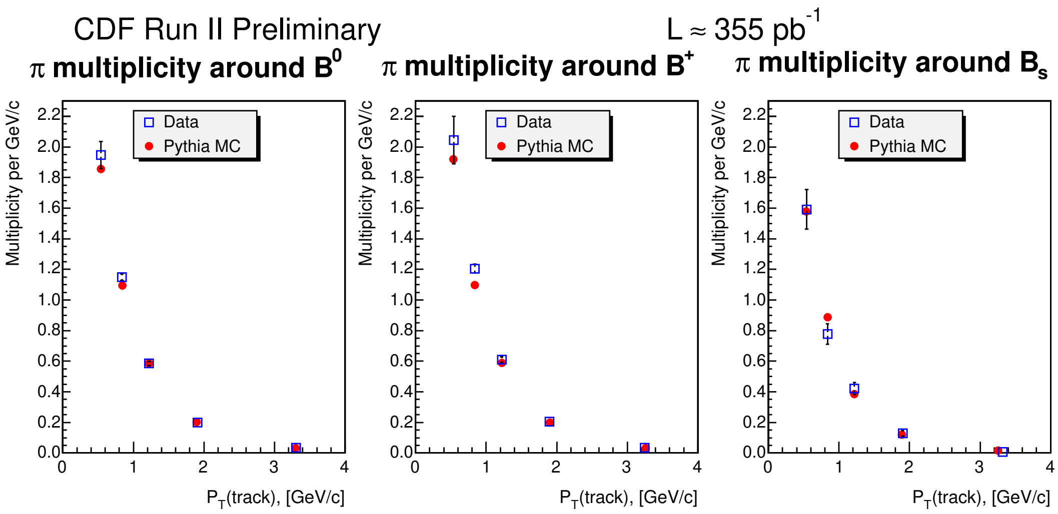

FIG. 5: Measured pion multiplicity in a sample of the tracks associated with B meson production shown as a function of the transverse momenta of these tracks.

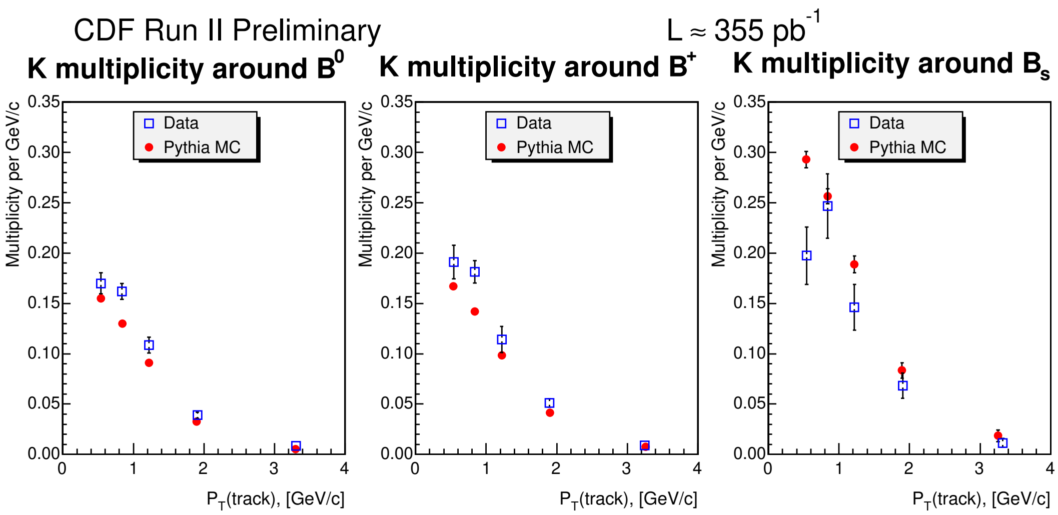

FIG. 6: Measured kaon multiplicity in a sample of the tracks associated with B meson production shown as a function of the transverse momenta of these tracks.

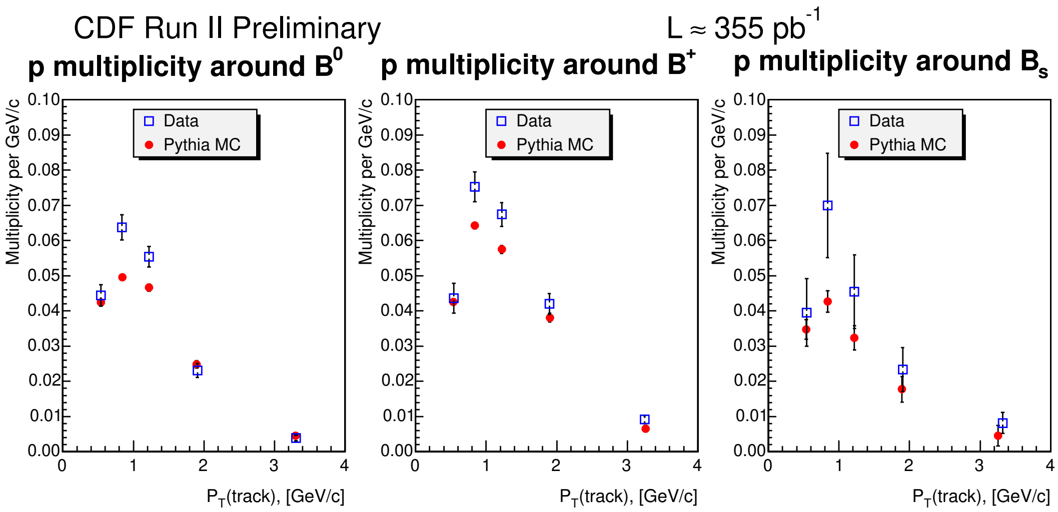

FIG. 7: Measured proton multiplicity in a sample of the tracks associated with B meson production shown as a function of the transverse momenta of these tracks.

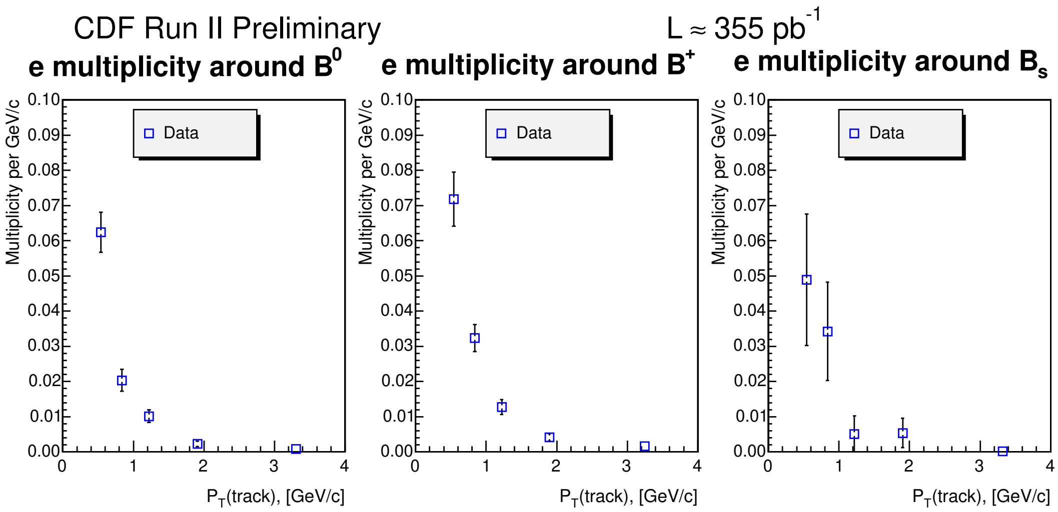

FIG. 8: Measured electron multiplicity in a sample of the tracks associated with B meson production shown as a function of the transverse momenta of these tracks.

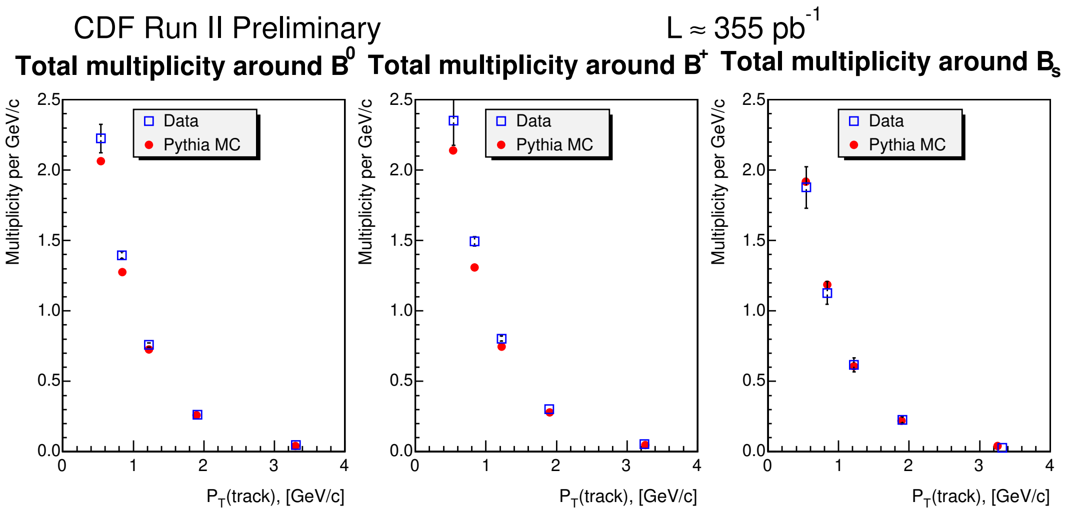

FIG. 9: Measured combined particle multiplicity in a sample of the tracks associated with B meson production shown as a function of the transverse momenta of these tracks.

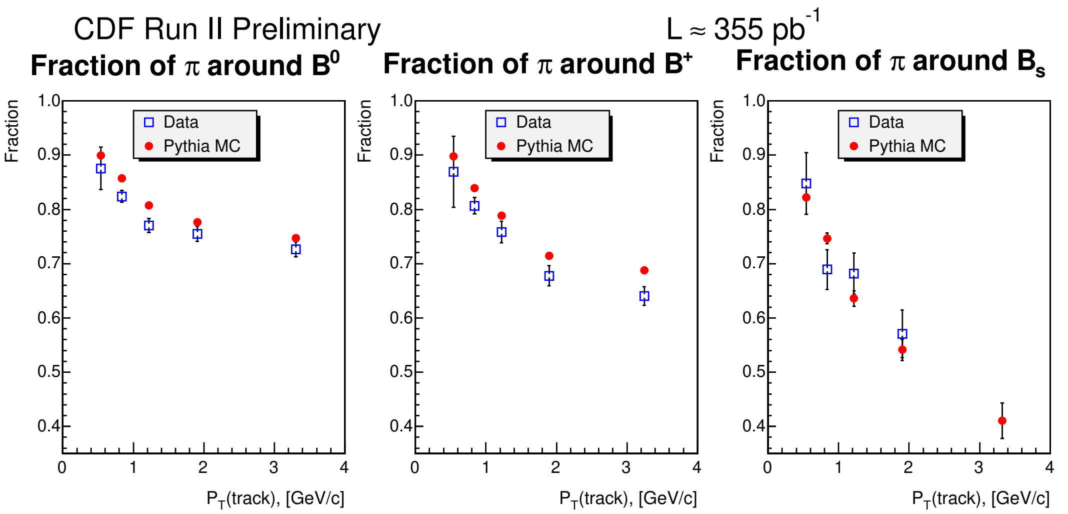

FIG. 10: Measured fraction of the pions in a sample of the tracks associated with B meson production shown as a function of the transverse momenta of these tracks.

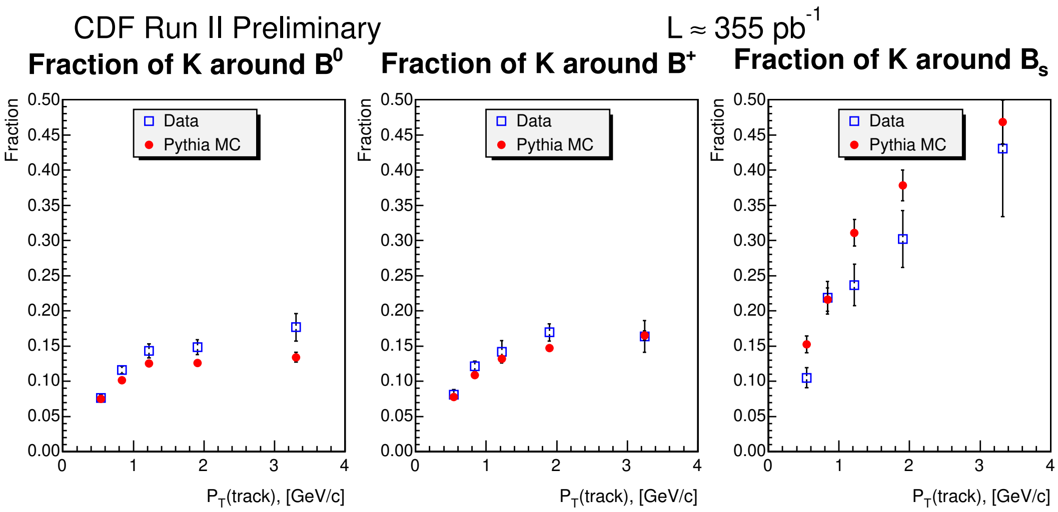

FIG. 11: Measured fraction of the kaons in a sample of the tracks associated with B meson production shown as a function of the transverse momenta of these tracks.

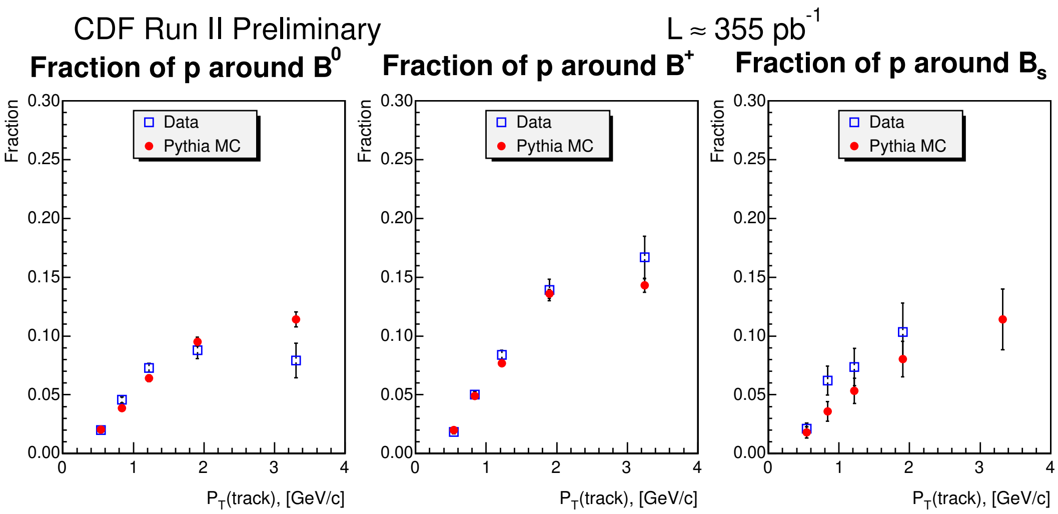

FIG. 12: Measured fraction of the protons in a sample of the tracks associated with B meson production shown as a function of the transverse momenta of these tracks.

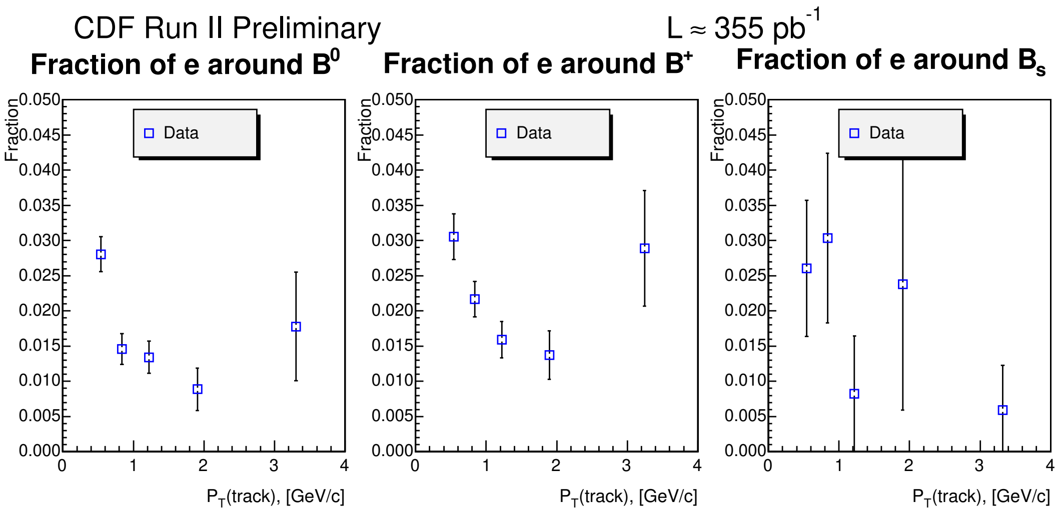

FIG. 13: Measured fraction of the electrons in a sample of the tracks associated with B meson production shown as a function of the transverse momenta of these tracks.